

## A Resonant-Cap Power Combiner for Two-Terminal Millimeter-Wave Devices

T. Bauer, J. Freyer, and M. Claassen

**Abstract**—A power combiner for three active two-terminal devices located under a common resonant cap is presented. An equivalent circuit with lumped elements describing the coupling between the devices is derived from a numerical finite-element simulation of the resonator. The applied monolithically integrated mounting technique for the active devices minimizes parasitic elements and gains high reproducibility and symmetry. Experimental results with GaAs IMPATT diodes on diamond heatsink of up to 500 mW at 91 GHz with a dc to RF conversion efficiency of 9.0% and excellent combining efficiency demonstrate the capability for power generation in the mm-wave region.

**Index Terms**—GaAs IMPATT oscillator, millimeter-wave power combiner, multiple device oscillator.

### I. INTRODUCTION

Solid-state oscillators are used in various fields of application, fostered by their advantages of, for example, low-input power requirements, low weight, small size, and the possibility of integration with modern semiconductor technology. One drawback, especially when proceeding toward near-millimeter-wave frequencies, is a lack of output power. To increase the output power of solid-state oscillators, a variety of power combining techniques has been developed. For the case of two-terminal devices an overview is given by Chang and Sun [1].

Sun *et al.* [2] have shown that power addition of two individual active devices under a common resonant cap in a V-band resonator is possible in principle. The devices were bonded with crossed gold-ribbons in ceramic pill packages. At elevated frequencies, however, the application of dielectric materials and of gold ribbons introduces unwanted parasitic elements [3], [4], which essentially determine the matching of the active devices and the load and generally reduce maximum output power and operating frequency. Additionally, the manual encapsulation of devices in a power combiner leads to a lack of symmetry, which severely deteriorates combining efficiency [5]. In 1994, Bauer and Freyer proposed an integrated mounting technique for three active devices [6] that minimizes the parasitic elements (due to the fact that dielectric materials and contact bondings are completely avoided) and provides a maximum of geometrical and, as we will show here, electrical symmetry.

### II. CHARACTERIZATION OF THE RESONATOR WITH A SCATTERING PARAMETER SIMULATION

Cap-resonators are in widespread use for oscillator structures and have been applied successfully by many authors [2]–[4] to match active two-terminal devices with low impedance to the relatively high impedance of rectangular waveguides. The device mounting technique in such resonators has to fulfill two major functions: enabling dc-voltage supply for the diodes and keeping the resonator cap in a certain distance above the waveguide bottom. Both are

Manuscript received December 4, 1995; revised September 23, 1996. This work was supported by the Deutsche Forschungsgemeinschaft (SFB 348).

The authors are with the Lehrstuhl für Allgemeine Elektrotechnik und Angewandte Elektronik, Technische Universität München, München 80290, Germany.

Publisher Item Identifier S 0018-9480(97)00280-9.

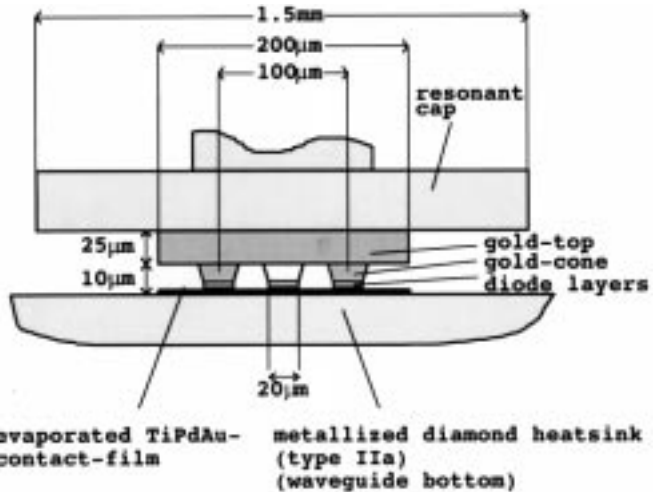


Fig. 1. Schematic cross section of the three-diode module with GaAs IMPATT diodes on diamond heatsink.

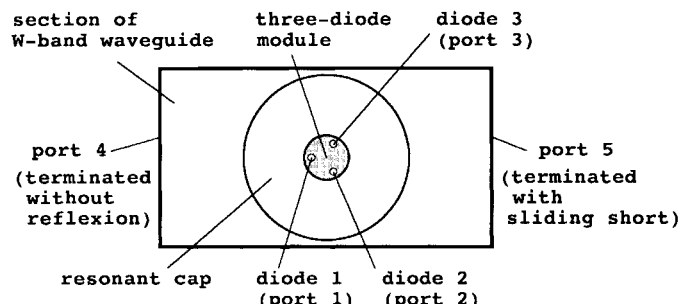


Fig. 2. Schematic top view of the waveguide mount.

satisfied by the centerpiece of the presented power combiner, the integrated three-diode module, depicted in Fig. 1. Three active diodes together with a gold-top compose a self-supporting structure to carry the resonator cap. No dielectrics are needed as in the case of standoff or quartz-ring mounted active devices.

To investigate the impedance matching of the new power combiner, the procedure suggested by Freyer *et al.* is applied [7]. The resonator shown schematically in Fig. 2 is simulated as a five-port system with HFSS (Hewlett Packard), three ports for the three devices (ports 1, 2, and 3), one port for power extraction (port 4), and one port for tuning with a sliding short (port 5). The distance of ports 4 and 5 from the center (2.0 mm) is chosen such that at both ports the fundamental  $H_{10}$  mode of the rectangular waveguide is dominant and higher order modes are negligible.

The simulations are carried out for a full-height W-band cap resonator with a cap diameter of 1.5-mm and 100- $\mu$ m distance between the single devices. At the position of each active device, a coaxial line is introduced to simulate coupling of the device to the resonator (ports 1, 2, 3). A comparison with an analytical solution of the radial-line/coaxial-line junction [8] proves that, with the help of the coaxial lines, the required input impedances at the diode ports (which are actually radial line entries) are nearly exactly obtained, if the inner diameter of the coaxial lines is chosen to be equal to the diode diameter of 20  $\mu$ m. An outer diameter of 30  $\mu$ m is used in the calculations, leading to a characteristic impedance  $Z_w$  of the coaxial lines of 24.2  $\Omega$ . Port 1 (diode 1) lies within the longitudinal

symmetry plane of the waveguide, whereas ports 2 and 3 are located symmetrically to this plane (Fig. 2). Together with the two rectangular ports (4, 5) for the waveguide entries, the  $5 \times 5$  scattering matrix  $\mathbf{S}^{(5)}$  of this five-port structure is calculated at different frequencies using HFSS.

Port 4 is terminated with an ideal absorber as load, i.e., without reflection ( $\rho_4 = 0$ ), whereas the reflection factor  $\rho_5$  at port 5 depends on the distance  $l$  of the sliding short plane. Considering these two conditions, the scattering matrix  $\mathbf{S}^{(5)}$  can analytically be reduced to a  $3 \times 3$ -type matrix  $\mathbf{S}^{(3)}$ , describing power flow between the three active devices and dissipation in the load. The analytical implementation of the sliding short reduces the numerical effort drastically, as only one finite-element calculation is necessary to characterize the whole system for all positions of the sliding short. The formula for reducing the  $S$ -matrix  $\mathbf{S}^{(n)}$  of type  $n \times n$  to the  $S$ -matrix  $\mathbf{S}^{(n-1)}$  of type  $(n-1) \times (n-1)$  by terminating port  $n$  with a reflection factor  $\rho_n$  is as follows:

$$S_{i,j}^{(n-1)} = S_{i,j}^{(n)} + \frac{S_{i,n}^{(n)} \cdot S_{n,j}^{(n)}}{\frac{1}{\rho_n} - S_{n,n}^{(n)}}, \quad i, j = 1, \dots, n-1. \quad (1)$$

This formula is applied twice to obtain the scattering matrix between the three active devices  $\mathbf{S}^{(3)}$ . From the relatively large magnitudes ( $\approx 0.3$ ) of the nondiagonal elements of  $\mathbf{S}^{(3)}$ , it follows that a strong coupling exists between the individual diodes, a prerequisite for synchronization [9]. The nonzero phases ( $\approx 50^\circ$ ) of the nondiagonal elements indicate that the three diodes are separated from the point of view of the electromagnetic field distribution, although the distances between them ( $100 \mu\text{m}$ ) are small compared to the free space wavelength of  $\lambda_0 = 3.3 \text{ mm}$  at 91 GHz.

The distances of  $100 \mu\text{m}$  between the devices in our experiment are chosen such that the devices are electrically strongly coupled and that at the same time the thermal interaction is weak [10]. For a low microwave frequency of 3 GHz, Rosen *et al.* reported on a multimesa mounting technique (diode diameters of  $150 \mu\text{m}$  and a spacing of  $300 \mu\text{m}$ ), in which, in contrast to our experiment, the devices are electrically not separated and can be treated as one large diode with improved thermal resistance [11]. In Rosen's experiment, all devices automatically operate in-phase, because they are arranged in a parallel circuit. In our oscillator, in-phase operation at a common frequency for the desired power combining is achieved with synchronization by mutual injection locking due to strong coupling.

Principally, the geometry of the mounting in Fig. 2 is asymmetrical concerning the three diodes, because the rectangular waveguide configuration is not radially homogeneous. In the scattering matrix  $\mathbf{S}^{(3)}$ , however, the electrical asymmetries are of the order of  $10^{-3}$ , which is comparable to the numerical error, and are neglected in the following. For example, the resonator is electrically highly symmetrical and therefore well suited for power combining [5].

A comparative calculation has been performed for three diodes located consecutively with  $100\text{-}\mu\text{m}$  distances in the longitudinal symmetry plane of the waveguide rather than on the corners of an equilateral triangle. The result is a difference of more than 10% in the relevant matrix elements. This confirms that the device configuration under the resonant cap is not arbitrary to achieve the symmetry necessary for high combining efficiency. The equidistant arrangement of devices on a circle is the optimum solution to obtain high symmetry.

### III. THEORETICAL DESCRIPTION OF POWER COMBINING WITH AN EQUIVALENT CIRCUIT

For a closer look at impedance matching, the description of the radio frequency (RF) circuit in terms of impedances is appropriate.

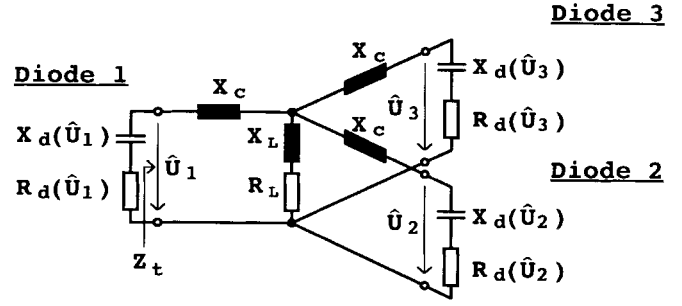


Fig. 3. Equivalent circuit representation of resonant structure with active devices.

To this end, the symmetrized scattering matrix  $\mathbf{S}^{(3)}$  is transformed to a  $3 \times 3$  impedance matrix:  $\mathbf{Z}^{(3)}$

$$\mathbf{Z}^{(3)} = Z_w \cdot (\mathbf{E}^{(3)} - \mathbf{S}^{(3)})^{-1} \cdot (\mathbf{E}^{(3)} + \mathbf{S}^{(3)}) \quad (2)$$

where  $\mathbf{E}^{(3)}$  is the  $3 \times 3$  unity matrix and  $Z_w$  is the characteristic impedance of the used coaxial lines.

From the elements of the matrix  $\mathbf{Z}^{(3)}$ , a symmetrical equivalent circuit is derived, which is illustrated in Fig. 3 together with the active devices. All three diodes are connected to a common load impedance  $R_L + jX_L$  by coupling reactances  $X_C$ . The values of the network elements are given in Fig. 4 as a function of the sliding short position. It is interesting that for a frequency range from 60 to 150 GHz, the coupling reactance  $X_C$  corresponds to a constant inductance  $L_C$  of about 4 pH, independent of frequency and sliding short distance.

Kurokawa [12] presented a theory for symmetrical multiple-device oscillators. For the three-diode structure depicted in Fig. 3, three eigenmodes of operation exist. In two destructive modes, the diodes oscillate with phase-shifts of  $120^\circ$ , so that the currents in the load cancel each other. Only the one constructive mode, in which all three diodes operate in phase, can transfer RF power to the load resistance. The RF design of the investigated oscillator forces in-phase operation, because the eigenfrequency of the destructive modes is above 140 GHz and is therefore outside the negative-resistance range of the diodes due to unavoidable losses at the contacts. A more detailed study on stability and in-phase operation is given elsewhere [13]. In the case of the in-phase mode, the total load impedance  $Z_t = jX_C + 3 * (R_L + jX_L)$  appears at each device terminal. Real and imaginary part of the total load impedance  $Z_t$  are given in Fig. 4.  $Z_t$  shows a favorable behavior, i.e., the imaginary part is nearly independent of the sliding short position and fixes the operating frequency at the desired value. The slow, continuous transition of the real part between 0 and  $1 \Omega$  allows exact and easy tuning for maximum output power.

The impedance  $Z_d(\hat{U}) = R_d(\hat{U}) + jX_d(\hat{U})$  of the applied active devices has been evaluated with a large-signal simulation for RF voltage amplitudes  $\hat{U}$  between 0 and 12 V at 90 GHz [14]. The real part  $R_d$  attains values between  $-1.9$  and  $0 \Omega$ , and the imaginary part  $X_d$  between  $-15.7$  and  $-13.6 \Omega$ . These values match well with the total load impedance  $Z_t$  at the terminals for the in-phase mode of operation.

### IV. EXPERIMENTAL RESULTS

For the implementation on diamond heatsink, single-drift flat-profile GaAs Impatt diodes with a 400-nm-wide active region ( $2 \times 10^{17} \text{ cm}^{-3} n\text{-doped}$ ) and diameters of  $20 \mu\text{m}$  have been used. The close spacing of the devices as compared to the free space wavelength leads to a high device density and allows to make use of a compact and simple resonator structure with only one sliding short for tuning, as usually applied for single-diode oscillators [3], [4].

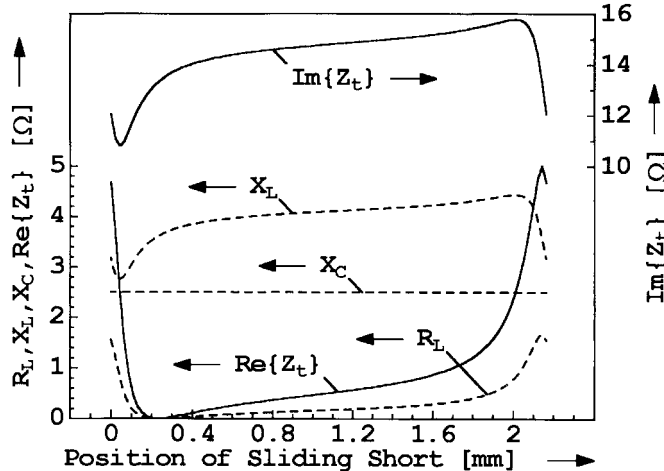


Fig. 4. Values of the network elements and total load impedance as functions of the sliding short position for 91 GHz.

The fabrication of the whole structure is similar to that reported for copper heatsink [6], except that the integral heatsink on the bottom of the devices is replaced by an evaporated TiPdAu contact-film of diameter 200  $\mu\text{m}$  with a thickness of 300 nm, as shown in Fig. 1. The whole structure with three devices is thermocompression bonded onto the metallized diamond heatsink. The maximum dc input power is about two times higher than on copper. As a consequence, the active device dc-current density could be raised up to 50  $\text{kA}/\text{cm}^2$ . The best result achieved is 500 mW output power at 91 GHz with a dc to radio frequency (RF) conversion efficiency of  $\eta = 9.0\%$ . The oscillation spectrum is absolutely clean and single moded, and up to the highest rf power levels a noise-to-carrier ratio better than  $-96$  dBc/Hz could be observed at a frequency of 500-kHz off-carrier.

Output power and efficiency are twice as high as compared to the results with the same device structure in a conventional resonator reported from Eisele [15] (250 mW at 91 GHz with  $\eta = 4.5\%$ ). Due to the application of small devices with resulting low thermal resistance, the conversion efficiency of our oscillator is comparable to the best published value from Tscherenitz and Freyer [4] (140 mW at 90 GHz with  $\eta = 10.4\%$ ).

If the experimental results are compared to that of a single diode mount with the same device structure and nearly the same diode diameter [4] (165 mW at 87 GHz with  $\eta = 8.6\%$  and a diameter of 21  $\mu\text{m}$ ), it is found that while the conversion efficiencies are comparable, the output power of the combiner is actually three times higher.

## V. CONCLUSION

The performance of a new mm-wave power combiner for waveguide cap-resonators is described. The maximum cw power output of the arrangement of three active devices under a common resonant cap is 500 mW at 91 GHz with 9.0% conversion efficiency, which is to the authors' knowledge the highest value of output power of oscillators with GaAs-devices reported at this frequency. Output power and efficiency attain both high values. Impedance matching is explained in terms of in-phase operation of three individual devices, which are strongly coupled by the RF circuit and therefore synchronize to a common frequency. An appropriate RF design of the oscillator—one that takes the effects of the separation of the diodes into account, i.e., multiple-device operation and prohibits the destructive modes—is necessary. The passive RF circuit is described with a numerical simulation of the resonator structure and validated with the diode impedances from a large-signal simulation. Monolithic integration of the mounting structure, together with a minimization of the parasitic

elements, leads on the one hand to good reproducibility and on the other hand to high electrical symmetry, essential for efficient power combining at mm-wave frequencies.

## ACKNOWLEDGMENT

The authors are grateful to H. Grothe for supplying the MBE-wafers. Technological advice from M. Tscherenitz is appreciated.

## REFERENCES

- [1] K. Chang and C. Sun, "Millimeter-wave power-combining techniques," *IEEE Trans. Microwave Theory Tech.*, vol. MTT-31, pp. 91–107, 1983.
- [2] C. Sun, E. Benko, and J. W. Tully, "A tunable high-power V-band Gunn oscillator," *IEEE Trans. Microwave Theory Tech.*, vol. MTT-27, pp. 512–514, 1979.
- [3] H. Eisele and J. Freyer, "Single-drift flat-profile GaAs IMPATT diodes at 90 GHz," *Electron. Lett.*, vol. 22, pp. 224–225, 1986.
- [4] M. Tscherenitz and J. Freyer, "GaAs modules for power generation at W-band frequencies," in *Proc. 23rd European Microwave Conf.*, 1993, pp. 446–447.
- [5] C. T. Rucker, G. N. Hill, N. W. Cox, and J. W. Amoss, "Symmetry experiments with four-mesa IMPATT diodes," *IEEE Trans. Microwave Theory Tech.*, vol. MTT-25, pp. 75–76, 1977.
- [6] T. Bauer and J. Freyer, "New mounting technique for two-terminal millimeter-wave devices," *Electron. Lett.*, vol. 30, pp. 868–869, 1994.
- [7] J. Freyer, B. Mayer, and M. Tscherenitz, "CAD for mm-wave resonators," in *Proc. 24th European Microwave Conf.*, 1994, vol. 1, pp. 273–278.
- [8] A. G. Williamson, "Radial-line/coaxial-line stepped junction," *IEEE Trans. Microwave Theory Tech.*, vol. MTT-33, pp. 56–59, 1985.
- [9] K. Kurokawa, "Injection locking of microwave solid-state oscillators," in *Proc. IEEE*, 1973, vol. 61, pp. 1386–1410.
- [10] T. Bauer and J. Freyer, "Optimization of mm-wave multiple-device oscillators," in *Proc. 21st Int. Conf. on Infrared and Millimeter Waves*, 1996, vol. CM2.
- [11] A. Rosen, H. Kawamoto, J. Klatskin, and E. L. Allen Jr., "Integrated TRAPATT diode arrays," *IEEE Trans. Microwave Theory Tech.*, vol. MTT-23, pp. 841–843, 1975.
- [12] K. Kurokawa, "The single-cavity multiple-device oscillator," *IEEE Trans. Microwave Theory Tech.*, vol. MTT-19, pp. 793–801, 1971.
- [13] T. Bauer and J. Freyer, "Analysis of a new millimeter wave power combiner," in *Proc. 25th European Microwave Conf.*, 1995, vol. 1, pp. 470–473.
- [14] L. Gaul, "Großsignal-und Stabilitätsanalyse von GaAs-Lawinendioden für Puls-Leistungsszillatoren im Millimeterwellen-bereich," Ph.D. dissertation, Technische Universität München, Germany, 1993.
- [15] H. Eisele, "GaAs W-band IMPATT diodes: The first step to higher frequencies," *Microwave J.*, pp. 275–282, May 1991.